

# Quantitative determination of the local structure of H<sub>2</sub>O on TiO<sub>2</sub>(110) using scanned-energy mode photoelectron diffraction

F. Allegretti <sup>a,1</sup>, S. O'Brien <sup>a</sup>, M. Polcik <sup>b</sup>, D.I. Sayago <sup>b</sup>, D.P. Woodruff <sup>a,\*</sup>

<sup>a</sup> Physics Department, University of Warwick, Coventry, W Midlands CV4 7AL, UK

<sup>b</sup> Fritz-Haber-Institut der Max-Planck-Gesellschaft, Faradayweg 4-6, D 14195 Berlin, Germany

Received 17 January 2006; accepted for publication 27 January 2006

Available online 20 February 2006

## Abstract

O 1s scanned-energy mode photoelectron diffraction has been used to determine the local structure of molecular water on TiO<sub>2</sub>(110). The adsorption site is found to be atop five-fold coordinated surface Ti atoms, confirming the results of published total energy calculations and STM imaging. The Ti–O<sub>w</sub> bondlength is found to be  $2.21 \pm 0.02$  Å, much longer than Ti–O bondlengths in bulk TiO<sub>2</sub> and for the formate (HCOO<sup>−</sup>) species adsorbed on this surface. This is consistent with relatively weak bonding, and in general agreement with total energy calculations, although all of the published calculations yield bondlengths somewhat longer than the experimental value. Structural optimisation based on the photoelectron diffraction data also provides some information on the associated substrate relaxation. In particular, the bondlength of the five-fold coordinated surface Ti atom to the O atom directly below shows the same contraction (relative to the bulk) as is found for the clean surface, reinforcing the picture of rather weak bonding of the water to this same Ti surface atom.

© 2006 Elsevier B.V. All rights reserved.

**Keywords:** Photoelectron diffraction; Chemisorption; Surface structure; Titanium dioxide; Water

## 1. Introduction

The (110) face of rutile phase TiO<sub>2</sub> is perhaps the most studied of all oxide surfaces [1–3] as a model system to investigate the range of catalytic applications of this material, of which one of the most interesting is the photochemical production of hydrogen from water, first discovered more than 30 years ago [4]. Most of the very extensive work on the interaction of water with this surface has recently been reviewed [3,5]. The extent to which H<sub>2</sub>O does, and should, dissociate to produce surface hydroxyl species on clean and well-ordered TiO<sub>2</sub>(110), remains a subject of controversy, at least between theory and experiment. However, experimentally it is well-established that molecular

water can be adsorbed on this surface intact at low temperatures.

Currently, however, there is no quantitative structural information regarding this adsorption, although STM studies have been interpreted in terms of molecular adsorption on the five-fold coordinated (i.e. under-coordinated) Ti atoms at the TiO<sub>2</sub>(110)(1 × 1) surface [6,7]. This is the site for molecular water adsorption which seems to be implicit in theoretical total energy calculations, although most of these [7–21] are primarily concerned with whether or not dissociation, to produce surface hydroxyl species, occurs on the perfect surface. This issue remains controversial; most of the earlier studies and some very recent ones predict facile dissociation on the perfect stoichiometric surface, and while a few calculations do reproduce the observed stability of adsorbed molecular water, the appropriateness of the methods used to achieve this remain a subject of debate [20,21]. Even in those papers which do explicitly identify a stable molecular water species, most

\* Corresponding author. Tel.: +44 2476523378; fax: +44 2476692016.

E-mail address: [d.p.woodruff@warwick.ac.uk](mailto:d.p.woodruff@warwick.ac.uk) (D.P. Woodruff).

<sup>1</sup> Now at Karl-Franzens-Universität Graz, Institut für Physik, Bereich für Experimentalphysik, Universitätsplatz 5, 8010 Graz, Austria.

do not give any adsorption bondlength information. However, amongst these many studies are four reported values for the Ti–O<sub>w</sub> bondlength from the surface Ti atom to the oxygen atom of the adsorbed water, namely 2.41 Å [10], 2.25 Å [13], 2.28 Å [16] and 2.32 Å [17]. These values of the Ti–O<sub>w</sub> bondlength values for H<sub>2</sub>O chemisorption are very much longer than Ti–O distances in bulk TiO<sub>2</sub> (1.94–1.99 Å) and, indeed, than the chemisorption bonds associated with formate (HCOO<sup>−</sup>) and OH adsorption on this surface (2.08 Å and 2.02 Å, respectively [22]), reflecting a weaker bond of rather different character for the intact water molecule. Because of this weaker bond, one might expect that the clean surface relaxations of the TiO<sub>2</sub>(110)(1 × 1) surface would be very little modified by the molecular water adsorption; an early theoretical study does report this conclusion [8], although a slightly later one suggests a substantial change in the relaxation of the five-fold coordinated Ti atom perpendicular to the surface by 0.14 Å [10]. None of the other theoretical studies cited above appears to address this question and prior to the work reported here there is no experimental information on this question.

The objective of the present work was to obtain quantitative experimental structural information on the local adsorption geometry of molecular water on the TiO<sub>2</sub>(110)(1 × 1) surface. Such data can provide important parameters with which to assess the quality of theoretical descriptions of the adsorbate–substrate interaction in this important system. The method we have used is scanned-energy mode photoelectron diffraction (PhD) [23], which we have previously applied successfully to determine the local adsorption structure on this same surface of coadsorbed formate and hydroxyl species resulting from interaction with formic acid [22]. The PhD technique exploits the coherent interference of the directly-emitted component of the outgoing photoelectron wavefield from a core level of an adsorbate atom with components of the same wavefield which are elastically backscattered by the nearby substrate atoms. By measuring the photoemission intensity in specific directions as a function of photon energy, the resulting changes in photoelectron energy, and thus photoelectron wavelength, cause specific scattering paths to switch in and out of phase with the directly-emitted component, leading to modulations in the intensity which depend on the relative emitter–scatterer location. Simulations of these PhD modulation spectra, including multiple scattering for the surrounding atoms in ‘guessed’ model structures, allow one to determine the local adsorption geometry by adjusting the model structure to optimise the theory–experiment agreement. One special virtue of the method is that it is not only element-specific, in that the binding energies of the core electrons are characteristic of the atomic identity of the emitter, but it is also chemical-state-specific through the so-called chemical shifts of these photoelectron binding energies. Thus, emission from atoms of the same element in different local environments can be distinguished by these shifts, and the associ-

ated PhD spectra can be analysed independently. This chemical-state specificity is particularly relevant in the present case, in which it is necessary to distinguish the O 1s photoemission from the adsorbed H<sub>2</sub>O from that from the underlying TiO<sub>2</sub>.

A brief report of the core conclusions of this investigation, namely the local adsorption site and Ti–O<sub>w</sub> bondlength, has appeared elsewhere [24]. Here we provide a far more complete account of the experimental details and structural analysis, and present important additional information on the structure, specifically the near-surface substrate relaxations.

## 2. Experimental details

The experiments were conducted in an ultra-high vacuum surface science end-station equipped with typical facilities for sample cleaning, heating and cooling. This instrument was installed on the UE56/2-PGM-2 beamline of BESSY II which comprises a 56 mm period undulator followed by a plane grating monochromator [25]. Different electron emission directions can be detected by rotating the sample about its surface normal (to change the azimuthal angle) and about a vertical axis (to change the polar angle). Sample characterisation in situ was achieved by LEED and by soft-X-ray photoelectron spectroscopy (SXPS) using the incident synchrotron radiation. Both the wide-scan SXPS spectra for surface characterisation, and the narrow-scan O 1s spectra used in the PhD measurements, were obtained using an Omicron EA-125HR 125 mm mean radius hemispherical electrostatic analyser, equipped with seven-channel parallel detection, which was mounted at a fixed angle of 60° to the incident X-radiation in the same horizontal plane as that of the polarisation vector of the radiation.

A clean well-characterised rutile TiO<sub>2</sub>(110) surface was prepared which gave a sharp (1 × 1) LEED pattern and a Ti 2p photoemission spectrum showing only a weak high kinetic energy shoulder. The main Ti 2p peaks are generally assigned to Ti in the 4+ charge state expected for a fully ionic stoichiometric bulk site and in the autocompensated surface (e.g. [26]), while any high energy shoulder is assigned to Ti in a 3+ state, most commonly attributed to the presence of surface oxygen vacancies. To achieve this surface the crystal was bombarded briefly with either Ar<sup>+</sup> or Ne<sup>+</sup> ions at an energy of 500 eV, followed by annealing in UHV at approximately 830 K. This surface was exposed to typically 10<sup>−6</sup> mbar s of H<sub>2</sub>O, at a partial pressure in the high 10<sup>−9</sup> mbar range, with a sample temperature of 125 K, and then heated to ~230 K and held at 190–200 K during measurement of the PhD spectra. This procedure ensured any excess (multilayer) water from the initial deposition was desorbed, and prevented (multilayer) re-adsorption from the residual vacuum which is always a slight hazard in working with water in a UHV chamber.

SXPS measurements in the range of the O 1s and Ti 2p peaks, and also of the valence band, were used to check

that the adsorbed layer remained stable during the PhD measurements. A key issue here is the possible influence of the incident synchrotron irradiation which has been suggested to be a major factor in the controversy concerning partial dissociation in water bilayers on Ru(0001) and Pt(111) [27–30], with clear evidence of partial photon-induced dissociation under certain conditions [27]. In our studies there was some evidence of photo-induced *desorption* as a result of exposure to the synchrotron radiation beam, but during the PhD data collection the water coverage remained stable, possibly due to a dynamic equilibrium with a low partial pressure of residual water, and there was no evidence of dissociation. In this context we should remark that in many undulator beamlines on third-generation synchrotron radiation sources, it is common to exploit the very low emittance to focus the radiation into small spots ( $\sim 50 \mu\text{m}$ ) at the sample. The associated very high flux density can greatly enhance the problem of radiation damage. In our case we deliberately mount our chamber  $\sim 1 \text{ m}$  beyond the focal point of the monochromated photon beam to ensure the spot on the sample is defocused to  $\sim 1 \text{ mm}$ , thereby greatly reducing the flux density. Relative to the literature report of radiation damage in water on Ru(0001) performed on a focussed beamline at the Advanced Light Source in Berkeley [27] we estimate our flux density at the sample to be  $10^4$ – $10^5$  times smaller, such that 1–2 h of radiation in our experiments (typical data collection times for PhD spectra) is roughly equivalent to  $\sim 0.1$ – $0.3 \text{ s}$  exposure in the ALS study.

Fig. 1 shows the changes in the O 1s SXPS spectrum associated with low temperature water dosing and subsequent annealing. A feature with a chemical shift of around 3.5 eV relative to the oxide peak is attributed to the presence of adsorbed molecular water on the surface; with in-

creased annealing temperatures and decreasing water peak intensity there is a shift in this peak of a few tenths of an eV away from the oxide peak, which we attribute to the desorption of the initial multilayer coverage. Somewhat surprisingly, we have been unable to find reports of XPS studies of the O 1s emission for low temperature deposition of water on  $\text{TiO}_2(110)$  with which to compare the photoelectron binding energies; there is a report of the appearance of the characteristic  $\text{H}_2\text{O}$  molecular valence features following such an exposure [31], but our own valence band SXPS spectra were not recorded to sufficiently high binding energy to reveal these peaks fully, but do show the appearance of the lower binding energy ( $\sim 10 \text{ eV}$ ) feature associated with molecular water. For room temperature water exposure, XPS measurements have been reported of a shoulder on the oxide O 1s peak with a smaller chemical shift of about 1.6 eV, that has been attributed to OH on the surface associated with water dissociation [26]; indeed, this attribution was also the basis of our earlier PhD structural study of coadsorbed formate and hydroxyl species on  $\text{TiO}_2(110)$  [22]. In our present experiments we see very little evidence for this shoulder after heating the water-covered surface to 270 K, possibly reflecting a very low density of surface oxygen defects for  $\text{H}_2\text{O}$  reaction. Our Ti 2p spectra showed no significant change in shape associated with the water adsorption or desorption, and in particular no evidence of ‘healing’ of the features associated with the weak  $\text{Ti}^{3+}$  feature which was reported for room temperature water exposure [26]. We should note, however, that these earlier reports of healing and surface OH creation involved very high exposures at room temperature (up to  $10^3 \text{ mbar s}$ ). Notice, though, that the spectrum of Fig. 1 obtained following annealing to 230 K, similar to our standard preparation approach for PhD measurements, does show some evidence of excess intensity between the molecular water and oxide peaks which could be attributed to coadsorbed OH. We will consider this feature further below.

One experimental parameter that is difficult to determine precisely is the water coverage used in our PhD structure determination. It has been suggested in some theoretical studies that this quantity may be significant in determining the stability of the intact molecule on the surface, with dissociation being particularly strongly favoured at coverages below 0.5 ML [32]. By comparing the intensity of the O 1s photoemission signal from the water adsorbate with that from the oxide substrate, and the attenuation in the substrate emission signal due to the water adsorbate, we have estimated the coverage assuming an attenuation length for the escaping electrons at 200 eV kinetic energy of 7–8 Å. There is a significant variation in the resulting value depending, in particular, on whether one uses measurement at normal emission or more grazing emission (after allowing, of course, for the longer escape distance). The calculations are also sensitive to the value of the attenuation length which is not known explicitly in  $\text{TiO}_2$  or the water overlayer. The coverage estimate therefore covers the

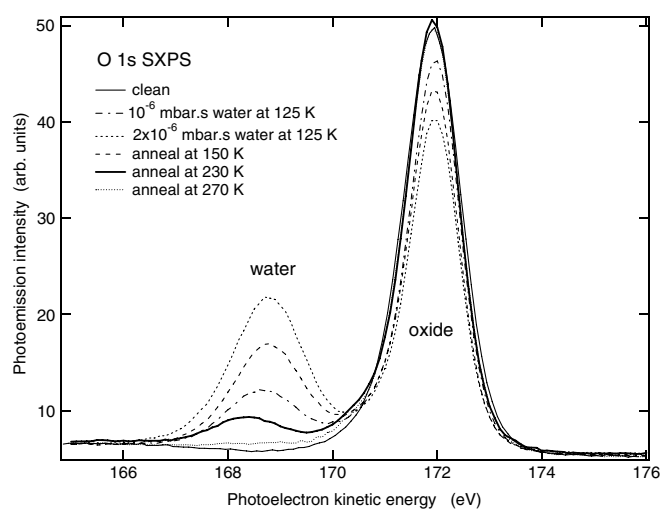


Fig. 1. Soft X-ray photoelectron spectra in the energy range of the O 1s emission recorded at a photon energy of 700 eV from a clean  $\text{TiO}_2(110)$  surface, and from the same surface following low temperature exposure to water and subsequent heating to successively higher temperatures. The two main component peaks due to emission from the  $\text{TiO}_2$  substrate, and from the adsorbed water, are labelled.

rather wide range of 0.45–0.90 ML (where 1 ML corresponds to the surface coverage of five-fold coordinated surface Ti atoms). We therefore conclude that the coverage is *not* significantly less than 0.5 ML, but cannot distinguish with confidence between  $\sim 0.5$  ML and  $\sim 1.0$  ML.

The PhD modulation spectra were obtained by recording a sequence of photoelectron energy distribution curves (EDCs) around the O 1s peaks at 4 eV steps in photon energy in the photoelectron kinetic energy range of approximately 50–315 eV for each of a number of different emission directions in the polar emission angle range from 0° (normal emission) to 60° in several azimuthal planes. Specifically, PhD spectra were obtained at polar angles of 0°, 10°, 20°, 30°, 40° and 60° in [001], at 5°, 10° and 20° in [112] and at 0°, 10°, 20°, 30° and 40° in [110]. These data were processed following our general PhD methodology (e.g. [23]) in which the individual EDCs are fitted by the sum of Gaussian peaks, a step and a template background. In the present case two different fitting procedures were used, one fitting the O 1s spectra to two Gaussian peaks (corresponding to those identified as associated with molecular water and the bulk oxide in Fig. 1), the second including an intermediate third Gaussian peak which might be associated with a coadsorbed OH species at low temperature. A key finding was that the PhD modulation spectra extracted from the molecular water component of the O 1s emission was essentially identical in these two different approaches. Somewhat surprisingly, the PhD modulation spectra obtained from the intermediate feature in the three-peak fit was essentially the same as for the oxide peak, rather suggesting that this apparent shoulder is not due to coadsorbed hydroxyl but, if it really is a discrete peak, is directly related to the oxide O atom emission. The important conclusion, however, is that the PhD structural data for the adsorbed molecular water are consistent, and apparently uninfluenced by the way the remainder of the O 1s spectra were fitted.

### 3. Results and structure determination

Structure determination in PhD is based on multiple scattering simulations for trial model structures which are compared with the experimental modulation spectra. These calculations were performed with computer codes developed by Fritzsche [33–35] that are based on the expansion of the final state wave-function into a sum over all scattering pathways which the electron can take from the emitter atom to the detector outside the sample. Key features are treatment of double and higher order scattering events by means of the reduced angular momentum expansion (RAME) and inclusion of the effects of finite energy resolution and angular acceptance of the electron energy analyser analytically. Anisotropic vibrations for the emitter atom and isotropic vibrations for the scattering atoms are also taken into account. The quality of agreement between the theoretical and experimental modulation amplitudes is quantified by the use of an objective reliability factor (*R*-

factor) defined [23] such that a value of 0 corresponds to perfect agreement and a value of 1 to uncorrelated data. Different model structures were initially tested on a grid-search of structural parameter, but this structural optimisation to locate the minimum *R*-factor was also aided with the help of an adapted Newton–Gauss algorithm. In order to estimate the errors associated with the individual structural parameters we use an approach based on that of Pendry which was derived for LEED [36]. This involves defining a variance in the minimum of the *R*-factor,  $R_{\min}$ : all parameter values giving structures with *R*-factors less than  $R_{\min} + \text{Var}(R_{\min})$  are regarded as falling within one standard deviation of the ‘best fit’ structure [37].

The experimental data used in this analysis comprise a sub-set of all the experimental PhD spectra. In general, these are selected to be those which show the strongest modulations and thus are the most statistically reliable, but it is also helpful to include as wide a range of different emission directions as possible. In the present case the modulation amplitudes were largest for those spectra recorded near-normal emission, the modulation amplitude decreasing with increasing polar emission angle; this behaviour is characteristic of an emitter site close to atop a strongly-scattering surface atom, which then contributes scattering particularly in the favoured 180° scattering angle. This general characteristic of the data strongly suggests that the O atom of the water does occupy the site above the five-fold coordinated Ti atoms of the TiO<sub>2</sub>(110) surface as previously suggested.

To test this hypothesis, calculations were first performed for the water O emitter atom at different heights above a five-fold coordinated surface Ti atom, assuming that the underlying TiO<sub>2</sub>(110) surface has a structure identical to the bulk. For the clean surface there are many theoretical calculations (see, e.g. [3]) and two experimental studies (by X-ray diffraction [38] and LEED [39]), all of which indicate significant (but quite varied) surface relaxations, but the bulk termination appears to be the most reasonable starting point for the adsorbate system, particularly as we do not know what surface relaxations occur in the presence of adsorbed water. Scattering from the H atoms was not included in the calculation, as previous studies of H-containing molecules (e.g. [40]) have indicated these weak scatterers give no significant contribution to the PhD modulations. The data set used for the theory–experiment comparison excluded only the experimental PhD spectra recorded at the largest polar emission angles which showed the weakest modulations. While the main structural analysis was performed using this subset of spectra, additional tests were conducted including some of the more weakly-modulated high-emission-angle spectra for the best-fit structural solutions to check that the absence of significant modulations in these directions was reproduced theoretically. The variation in the *R*-factor with Ti–O<sub>w</sub> interlayer spacing obtained from the initial calculations on the bulk-terminated substrate is shown in Fig. 2. The presence of three distinct minima at different interlayer spacings is

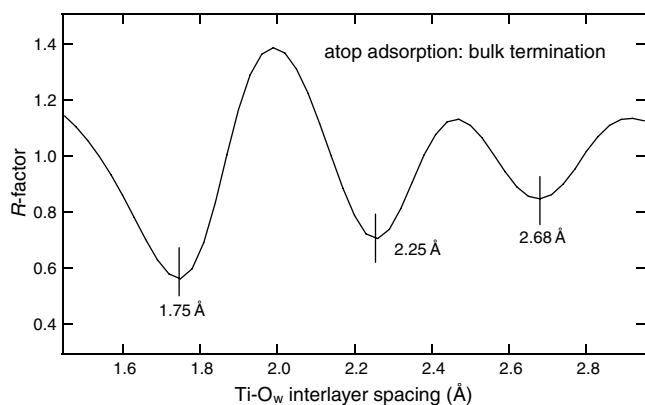


Fig. 2. Variation of the  $R$ -factor, a measure of the quality of theory–experiment agreement in the PhD spectra, with the height of the oxygen emitter atom in adsorbed  $\text{H}_2\text{O}$  above the five-fold coordinated surface Ti atom in  $\text{TiO}_2(110)$ , for calculations assuming that the  $\text{TiO}_2$  surface is described by an ideal termination of the bulk structure.

characteristic of both the PhD and quantitative LEED techniques and has been discussed in detail elsewhere [41,42]. Fig. 3 shows a comparison of the experimental PhD spectrum recorded at normal emission in the [001] azimuth with the results of the multiple scattering calculations for values of the  $\text{Ti-O}_w$  interlayer spacing corresponding to the three  $R$ -factor minima. Each shows a single dominant periodicity which can be attributed to the scattering path-length difference associated with the  $180^\circ$  scattering from the nearest-neighbour Ti atom, equal to twice the  $\text{Ti-O}_w$  bondlength. As this bondlength (and thus the scattering path-length difference) increases, the periodicity of the modulations decreases. There are three values of the bondlength for which the periodicity approximately matches that of the experimental spectrum as well as placing the peaks at approximately the correct energy;

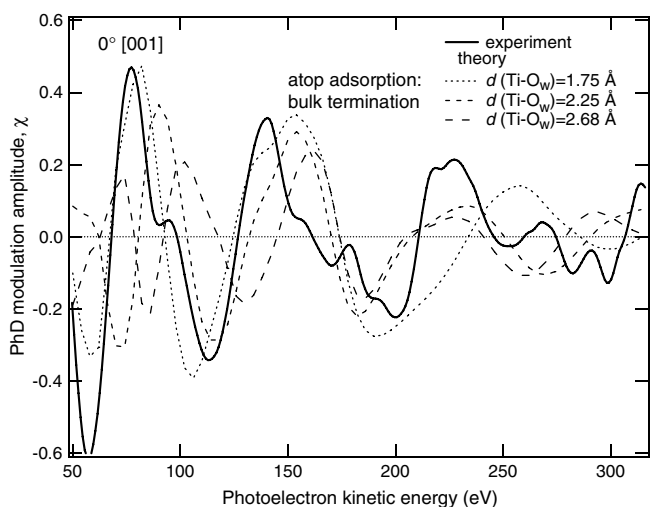


Fig. 3. Comparison of the experimental O 1s PhD spectra recorded from  $\text{H}_2\text{O}$  adsorption on  $\text{TiO}_2(110)$  at normal emission, with the results of calculations of this spectrum for the structures associated with the three  $R$ -factor minima seen in Fig. 2.

for intermediate bondlength values, the relative energies of the experimental and theoretical modulations shift into anti-phase locations and the  $R$ -factor increases to values greater than unity. Notice, though, that inspection of the three theoretical spectra in Fig. 3 suggests that the periodicity most closely matches that of the experiment for the intermediate bondlength value of 2.25 Å, despite the fact that the lowest value of the  $R$ -factor occurs for the shortest bondlength of 1.75 Å, probably because the strong lowest-energy modulation of this spectrum fits the absolute energy of the feature in the experimental data better. Of course, none of these minimal  $R$ -factor values corresponds to acceptable solutions, for which we typically expect a value of 0.3 or less. However, based on this first-order fitting we may anticipate that the best structural solution is likely to involve atop site adsorption with a  $\text{Ti-O}_w$  bondlength around 1.75 Å or 2.25 Å. The third minimum is very shallow, clearly gives a poor fit to the PhD modulation period in Fig. 3, and also corresponds to an implausibly-long bondlength.

Clearly, a more complete structural optimisation is required to establish a convincing level of theory–experiment agreement and to distinguish the two distinct possible bondlength ranges in an objective fashion. The latter issue is of particular importance because we have already remarked that theoretical total energy calculations for this weak adsorption system indicate a  $\text{Ti-O}_w$  bondlength associated with the water which is very significantly larger than the equivalent bondlengths in the bulk oxide. Indeed, a comparison of the experimental O 1s normal emission PhD spectrum of Fig. 3 with the equivalent experimental spectrum recorded from the coadsorbed formate and hydroxyl species on this surface [22] shows that these two spectra are almost exactly in antiphase, with maxima of one corresponding to minima of the other. The normal emission spectrum from coadsorbed formate and OH is dominated by the emission from the formate O atoms which occupy sites near atop the five-fold coordinated surface Ti atoms at a  $\text{Ti-O}_{\text{HCOO}}$  interlayer spacing of 2.06 Å, entirely consistent with a significantly longer or shorter value in the water adsorption system. However, it is important to establish which of these alternative interpretations is correct.

To establish this, a far more exhaustive set of multiple scattering PhD calculations was performed in which a range of different relaxations, both perpendicular and parallel to the surface, was considered for all the Ti and O atoms in the outermost two layers (Fig. 4). This search of combinations of structural parameters was conducted starting from each of the two very distinct  $\text{Ti-O}_w$  distances of 1.75 Å and 2.25 Å. In each case vibrational amplitudes (including anisotropy for the emitter atom vibrations) were also optimised. For the shorter adsorption bondlength this produced a reduction of the  $R$ -factor to 0.32, with the  $\text{Ti-O}_w$  bondlength being optimised at 1.70 Å, but this solution also involved unreasonably large values of the mean-square vibrational amplitude of the O emitter atom in excess of

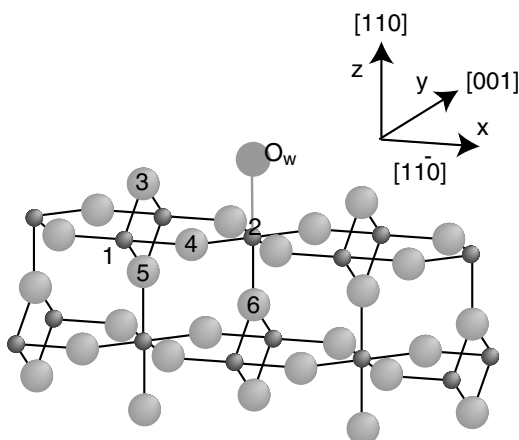


Fig. 4. Schematic perspective view of the  $\text{TiO}_2(110)$  surface with numerical labels (used in Table 1) for some of the inequivalent atoms. Ti atoms are represented by the smaller darker spheres than those representing O atoms. The oxygen atom of adsorbed  $\text{H}_2\text{O}$  is shown labelled  $\text{O}_w$  (while the associated H atoms are not shown).

$0.10 \text{ \AA}^2$  (and hence root-mean-square values in excess of  $0.3 \text{ \AA}$ ). By contrast, similar optimisation of the longer  $\text{Ti}-\text{O}_w$  bondlength structure led to an  $R$ -factor value of  $0.150$  with the  $\text{Ti}-\text{O}_w$  distance being  $2.21 \text{ \AA}$ , while the associated value of the mean-square vibrational amplitude of the emitter was far more reasonable at  $0.05 \text{ \AA}^2$  (quite similar to the value found for another weakly chemisorbed atop molecule, namely  $\text{NH}_3$  on  $\text{Ni}(111)$  [43]). Clearly the  $R$ -factor value for this second structure not only falls well in the range required for an acceptable solution, but is also so much smaller than the value for the shorter bondlength solution, that the shorter bondlength model can be excluded; specifically, the variance in  $R$  is  $0.020$  while the difference between the two minimum  $R$ -factor values is seven times this variance. As shown in Fig. 5, the resulting match of the simulated PhD spectra to the experimental spectra is

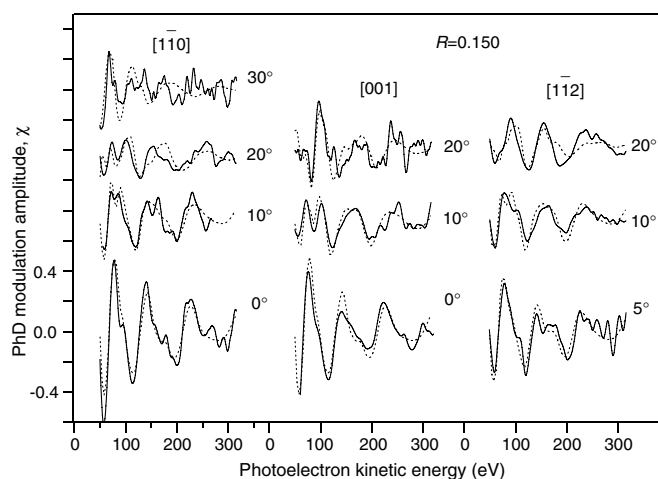


Fig. 5. Comparison of the full set of experimental O 1s PhD spectra (full lines) from adsorbed  $\text{H}_2\text{O}$  on  $\text{TiO}_2(110)$  used in the structural optimisation, with the results of the calculations (dashed lines) for the best-fit surface geometry as detailed in Table 1.

good for the best-fit structure, as may be anticipated by the low value of the  $R$ -factor.

Two important factors need to be recognised in considering the information to be gained from this optimisation regarding the near-surface relaxation of the  $\text{TiO}_2(110)$  surface. The first is that because the PhD technique uses a local source of electrons—namely the adsorbate emitter atom—the structural information provided is intrinsically local in character. Although proper convergence of the multiple scattering simulations typically necessitates including scattering from a cluster of 1000 atoms or so, the individual scattering contributions from the more distant atoms are very small. This is both a strength and a weakness of the method. It may be relatively straightforward to identify the local adsorption site and to determine the distances of the adsorbate emitter atom to the nearest-neighbour substrate atoms with excellent precision, but the precision with which more distant neighbours can be determined degrades sharply with increasing distance from the emitter, particularly if these neighbours are far-removed from  $180^\circ$  scattering geometries in the experimental data set. The second point is that there remains significant controversy over the details of the relaxation of even clean  $\text{TiO}_2(110)$ . Until recently there was only one experimental determination of this relaxation, using surface X-ray diffraction [38], and some of the parameter values obtained differ significantly from those of the many theoretical total energy calculations, e.g. [44–50] (although there is also significant variation in these theoretical studies). Very recently a new experimental study by quantitative LEED, which also presents new theoretical results [39], shows better theory/experiment consistency, but it is probably still premature to regard this issue as fully resolved.

Fig. 4 shows a schematic diagram of the outermost few atomic layers of the  $\text{TiO}_2(110)$  surface with an adsorbed water molecular represented by its oxygen emitter atom,  $\text{O}_w$ . The near-surface Ti (small dark spheres) and O atoms (larger shaded spheres) are numbered for convenient identification (cf. [22]). Although our calculations explored possible movements of all the atoms in the outermost two layers of the  $\text{TiO}_2$  surface, mainly perpendicular to the surface, the results proved very insensitive to many of these displacements. By far the most crucial parameter is the  $\text{Ti}-\text{O}_w$  distance, so it is important in identifying the influence of displacements of atoms in the surface away from the bulk-terminated positions to avoid the effects of strong coupling to this most sensitive parameter. For example, if one wishes to identify the sensitivity of the PhD results to the relaxation of the five-fold coordinated Ti atom (atom 2 in Fig. 4) within the surface, it is necessary to move both the emitter and this Ti atom simultaneously relative to the rest of the crystal; moving the Ti atom alone changes the  $\text{Ti}-\text{O}_w$  distance and so leads to a strong change in the  $R$ -factor which is largely unrelated to the shift of the Ti atom with respect to the underlying bulk. By contrast, determining the sensitivity to other substrate atom displacements can be achieved simply by moving these atoms within the

Table 1

Displacements of the near-surface Ti and O atoms in TiO<sub>2</sub>(110) relative to an ideal bulk-terminated structure, and the Ti–O<sub>w</sub> bondlength values, for the two lowest *R*-factor structures found in this study of molecular water adsorption on this surface

| Atom or bondlength            | Parameter              | Clean surface |              |       |         | Water adsorption—this study |                           |
|-------------------------------|------------------------|---------------|--------------|-------|---------|-----------------------------|---------------------------|
|                               |                        | SXRD          | LEED         | HF    | DFT-LDA | Best-fit <i>R</i> = 0.150   | Good-fit <i>R</i> = 0.157 |
| Ti(2)–O <sub>w</sub> distance | $d(\text{Ti–O}_w)$ (Å) | –             | –            | –     | –       | 2.21 ± 0.02                 | 2.21 ± 0.02               |
| Ti(2), five-fold coord.       | $\Delta z_2$ (Å)       | –0.16 ± 0.05  | –0.19 ± 0.03 | –0.17 | –0.17   | 0.27 ± 0.04                 | –0.39 ± 0.04              |
| O(4), surface planar          | $\Delta x_4$ (Å)       | –0.16 ± 0.08  | –0.17 ± 0.15 | 0.11  | 0.13    | –0.22 ± 0.14                | –0.24 ± 0.14              |
|                               | $\Delta z_4$ (Å)       | 0.05 ± 0.05   | 0.27 ± 0.08  | –0.06 | –0.06   | 0.48 ± 0.06                 | –0.18 ± 0.06              |
| O(6), below five-fold Ti      | $\Delta z_6$ (Å)       | 0.00 ± 0.08   | 0.00 ± 0.08  | –0.02 | –0.02   | 0.42 ± 0.07                 | –0.22 ± 0.07              |

Only parameter values found to be significant on the basis of their estimated precision are shown. The atom numbers used in the parentheses and suffices of the parameters are as defined in Fig. 4. Also shown are some clean surface values taken from the SXRD and LEED experiments [38,39] and two different (Hartree–Fock and density functional theory) total energy calculations [50].

scattering cluster with all other structural parameter values fixed at the previously-optimised values.

The results of these investigations show that, apart from the strong sensitivity to  $d(\text{Ti–O}_w)$ , the PhD spectra are mainly sensitive to the displacements of the five-fold coordinated nearest-neighbour Ti atom (atom 2 in Fig. 4), the O atoms within this surface layer (atom 4), and the oxygen atom directly below the five-fold coordinated Ti atom (atom 6). This sensitivity can be attributed to the fact that these are the substrate atoms closest to the emitter or most nearly in the 180° scattering geometry for near-normal emission, the geometry giving the strongest PhD modulations. The calculations are particularly sensitive to the location of the deeper-lying oxygen atom 6 (Fig. 4), possibly due to the back-scattering from this atom being enhanced by forward-focussing of the O 1s photoelectrons from the water molecule by the intervening five-fold coordinated Ti atom. The sensitivity to the location of the more distant bridging surface O atoms (atom 3 in Fig. 4) is poor. For many of the other individual substrate atoms (e.g the lower bridging O atom labelled 5, the six-fold coordinated surface layer Ti atoms labelled 1, or any of the other second layer Ti and O atoms) any position led to an *R*-factor value within the variance; i.e. it was even possible to remove such atoms completely without producing a formally unacceptable change in the *R*-factor.

While this structural optimisation phase provided a very clear identification of the correct Ti–O<sub>w</sub> bondlength for the adsorption structure, careful checks on the dependence of the *R*-factor on individual structural parameter values, required to determine the precision of these parameters, led to the discovery of a second set of relaxation parameter values with an *R*-factor value of 0.157, within the variance of *R* for the best-fit structure. The structural parameter values of these two solutions, labelled ‘best-fit’ and ‘good-fit’, are given in Table 1 which also includes the values of these same relaxation parameters for the clean surface according to the two experimental determinations [38,39] and the results of some of the most recent theoretical calculations by different methods [39,50]. Notice that Table 1 shows atomic displacements relative to the ideally-terminated bulk sites, following the format used in earlier experimental and theoretical studies of the TiO<sub>2</sub>(110) surface structure; as we

will show below, this may not be the most appropriate way to present the results of the present measurements. The perpendicular relaxations of the two different solutions, ‘best-fit’ and ‘good-fit’, are very different, and at first glance it seems puzzling that such different solutions can each appear to have quite high precision. More careful consideration, however, shows that these two solutions differ by a rigid shift of all of the perpendicular relaxations by almost exactly 0.6 Å. If we now bear in mind that the structural parameters which really matter in PhD are the locations of the scatterer atoms to the (O<sub>w</sub>) emitter atom, we see that the two alternative solutions correspond to almost identical positions of these outermost layer TiO<sub>2</sub> atoms relative to the emitter, but differ in the location of these surface atoms to the underlying bulk.

To explore this observation further, an additional set of calculations was performed in which the O<sub>w</sub> emitter atom and the complete set of first-layer TiO<sub>2</sub> atoms (including O(6) directly below the five-fold coordinated Ti atoms) were displaced rigidly perpendicular to the surface relative to the underlying bulk. Fig. 6 shows the results of this calculation in the form of a plot of the *R*-factor as a function of the perpendicular displacement of the surface layer above the underlying bulk relative to the position corresponding to the best-fit solution (as shown in Table 1).

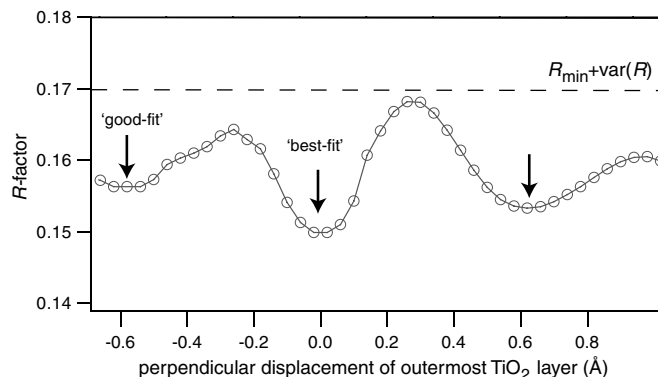


Fig. 6. Variation of the *R*-factor with the displacement of the outermost TiO<sub>2</sub> surface layers (including the O atom directly below the five-fold coordinated surface Ti atom) relative to the value for the best-fit structure of Table 1.

Table 2

Interlayer spacing changes from the five-fold coordinated surface Ti atom (Ti(2)) to the outermost O atoms in TiO<sub>2</sub>(1 1 0), relative to those in an ideal bulk-terminated structure

| Interlayer spacing changes relative to five-fold coordinated surface Ti atom (Ti(2)) |                     |                  |                  |       |         |                             |                      |
|--|---------------------|------------------|------------------|-------|---------|-----------------------------|----------------------|
| Atom   | Parameter           | Clean surface    |                  |       |         | Water adsorption—this study |                      |
|  |                     | SXRD             | LEED             | HF    | DFT-LDA | Best-fit $R = 0.150$        | Good-fit $R = 0.157$ |
| O(4), surface planar   | $\Delta z_{24}$ (Å) | $-0.21 \pm 0.07$ | $-0.46 \pm 0.09$ | -0.11 | -0.11   | $-0.21 \pm 0.07$            | $-0.21 \pm 0.07$     |
| O(6), below 5-fold Ti  | $\Delta z_{26}$ (Å) | $-0.16 \pm 0.09$ | $-0.19 \pm 0.09$ | -0.15 | -0.15   | $-0.15 \pm 0.08$            | $-0.17 \pm 0.08$     |

Values are given for the two lowest  $R$ -factor structures found in this study of molecular water adsorption on this surface and for the clean surface according to the SXRD and LEED experiments [38,39] and two different (Hartree–Fock and density functional theory) total energy calculations [50]. Spacings for the bridging surface oxygen atoms are not included as the estimated errors for the location of this atom are larger than the optimal values of the displacements.

Two important results emerge from Fig. 6. One is that not only is the deepest  $R$ -factor minimum at the relaxation corresponding to the best-fit structure, but there are also local minima corresponding both to shifting the outermost layer closer to the substrate by  $\sim 0.6$  Å (the ‘good-fit’ solution of Table 1) and to displacing the outer layer further from the substrate by  $\sim 0.6$  Å. Indeed, this third minimum is actually deeper than corresponding to the ‘good-fit’ structure, despite the implied surface layer expansion being implausibly large ( $\sim 0.8$  Å). The second feature shown by Fig. 6 is that all the layer spacing values explored in this graph have  $R$ -factor values less than the sum of the minimum value and its variance, as shown by the dashed line in Fig. 6. This means that there is no formal significance to any of the layer relaxations of Table 1 when expressed as displacements relative to the underlying bulk. The displacements and their associated precision values reported in Table 1 are significant, however, when expressed as positions relative to the O<sub>w</sub> emitter atom. Moreover, because the precision of the Ti–O<sub>w</sub> nearest-neighbour bondlength value is high ( $\pm 0.02$  Å), we can also express these outermost layer relaxations rather precisely with respect to the five-fold coordinated nearest-neighbour Ti atom within the surface layer. Table 2 shows these values for the two solutions of the water-covered surface found here, and for the experimental and some theoretical values for the clean surface. This table, which now involves far more meaningful parameter values and good precision, shows far more consistency both within our own results and with the clean surface values. In particular, the significant reduction (relative to the bulk) of the distance between the five-fold coordinated surface Ti(2) atom (Fig. 4) and the O(6) atom directly below it is found to be identical, within the experimental precision, for the water-covered surface and all the clean surface results. There is significantly more scatter, however, in the buckling between the Ti(2) and O(4) atoms which are coplanar in the bulk; curiously, it is the most recent (LEED) experimental result [39] for the clean surface which is least consistent with the theoretical values for this parameter; our own value for the water-covered surface is identical to the old SXRD [38] experimental value for the clean surface, both of which are larger, by a

formally significant amount, than the two theoretical clean surface values. One might ask if the experimental clean surface values could be influenced by contamination of adsorbed molecular water, but the SXRD study which agrees best with our results for a water-covered surface appears to have been performed at room temperature where water adsorption is not possible. By contrast, the LEED study was performed at low temperature, but this experiment yields results in poor agreement with both clean surface theory and our experimental result for the water-covered surface.

#### 4. Conclusions

Our structure determination for molecular water on TiO<sub>2</sub>(1 1 0) using O 1s scanned-energy mode photoelectron diffraction provides clear confirmation of the adsorption site, atop five-fold coordinated surface Ti atoms, deduced from total energy calculations and STM images. We also show that the Ti–O<sub>w</sub> bondlength is  $2.21 \pm 0.02$  Å, much longer than Ti–O bondlengths in bulk TiO<sub>2</sub> and for the formate species adsorbed on this surface, a result in good qualitative agreement with all total energy calculations. The molecular water is clearly relatively weakly bonded and the longer Ti–O distance reflects this fact. However, it is perhaps significant that all the theoretically-calculated values of this distance— $2.41$  Å [10],  $2.25$  Å [13],  $2.28$  Å [16] and  $2.32$  Å [17], are larger than the experimental value of  $2.21$  Å by significantly more than the estimated experimental error of  $\pm 0.02$  Å, although for one of these values ( $2.25$  Å [13]) the level of disagreement is modest. In our earlier determination of the adsorption geometries of CO, NO and NH<sub>3</sub> on NiO(100) we identified a very clear failure of existing theoretical treatments of this surface, with theoretical molecule-surface bondlengths of up to  $0.79$  Å too large [51]. However, NiO is generally regarded as an extremely difficult material to model well theoretically, and this problem continues to attract considerable effort [52]. By contrast, theoretical descriptions of the properties of TiO<sub>2</sub> are generally regarded as rather more reliable (albeit not without detailed controversy) and the experimental chemisorption bondlengths for coadsorbed formate and hydroxyl



species on this surface [22] proved to be in excellent agreement with current theory. Of course, these species form strong chemisorption bonds, whereas molecular water is much more weakly bonded. It seems that in this case theory significantly overestimates the associated adsorption bondlength, and presumably underestimates the bonding strength. As we have pointed out previously [24] this discrepancy may have a broader significance. A major controversy in the theoretical treatment of the interaction of water with ideal stoichiometric  $\text{TiO}_2(110)$  concerns the stability of the adsorbed molecular species, with many calculations predicting facile dissociation not seen experimentally. If theory fails to correctly describe the bonding of molecular water on this surface (as reflected by the long  $\text{Ti}-\text{O}_w$  bondlengths), then it is perhaps not surprising that the same theories fail to obtain the correct relative energies of transition states to dissociation. In this context it is perhaps significant that of the four theoretical papers which do report  $\text{Ti}-\text{O}_w$  bondlengths (listed above), the only one which predicts a stable molecular adsorbate is also the one which gives a bondlength value closest to our experimental result. Of course, there are other, more recent, theoretical studies that find stable molecular adsorption, but in these cases the  $\text{Ti}-\text{O}_w$  bondlength values have not, so far, been reported.

Our complete structural optimisation also provides some information on the associated substrate relaxation. The local character of the PhD technique means that the results are not very sensitive to the location of more distant substrate atoms or those far-removed from the favoured  $180^\circ$  backscattering geometry near-normal emission. A particular consequence of this is that the results do show significant sensitivity to the relative positions of some of the nearest-neighbour substrate atoms, but because the sensitivity to the location of deeper-lying substrate atoms is low, the surface relaxations cannot be expressed precisely in terms of atomic displacements relative to the bulk. However, some of the relative displacements we can detect are the ones of most interest in terms of the response of the surface to the bonding of the water. In particular, we find a clear reduction relative to the equivalent bulk value in the bondlength between the five-fold coordinated surface Ti atoms to which the water is bonded and the O atoms immediately below them. The value we find is essentially identical to that reported for the clean surface on the basis of both experimental and the most recent theoretical studies. On the clean surface this bondlength reduction can readily be assigned to the under-coordination of the surface Ti atoms; the fact that it remains essentially unchanged even when the water adsorbs onto this same Ti atom presumably reflects the weakness of this local adsorption bonding. We also obtain a value for the buckling between the five-fold coordinated Ti atoms and the O atoms within the same layer; in this case, however, large discrepancies in reported values of this parameter for the clean surface prevent us drawing any conclusions regarding the influence of the adsorbed water.

## Acknowledgements

The authors acknowledge the financial support of the Physical Sciences and Engineering Research Council (UK) and of the Deutsche Forschungsgemeinschaft through the Sonderforschungsbereich 546.

## References

- [1] V.E. Henrich, P.A. Cox, *The Surface Science of Metal Oxides*, Cambridge University Press, Cambridge, 1996.
- [2] D.P. Woodruff (Ed.), *The Chemical Physics of Solid Surfaces, Oxide Surfaces*, vol. 9, Elsevier, Amsterdam, 2001.
- [3] U. Diebold, *Surf. Sci. Rep.* 48 (2003) 53.
- [4] A. Fujishima, K. Honda, *Nature* 238 (1972) 37.
- [5] M.A. Henderson, *Surf. Sci. Rep.* 46 (2002) 1.
- [6] I.M. Brookes, C.A. Muryn, G. Thornton, *Phys. Rev. Lett.* 87 (2001) 266103.
- [7] R. Schaub, P. Thostrup, N. Lopez, E. Lægsgaard, I. Stensgaard, J.K. Nørskov, F. Besenbacher, *Phys. Rev. Lett.* 87 (2001) 266104.
- [8] J. Goniakowski, M.J. Gillan, *Surf. Sci.* 350 (1996) 145.
- [9] P.J.D. Lindan, N.M. Harrison, J.M. Holender, M.J. Gillan, *Chem. Phys. Lett.* 261 (1996) 246.
- [10] M. Casarin, C. Maccato, A. Vittadini, *J. Phys. Chem. B* 102 (1998) 10745.
- [11] D. Vogtenhuber, R. Podloucky, J. Redinger, *Surf. Sci.* 402–404 (1998) 798.
- [12] P.J.D. Lindan, N.M. Harrison, M.J. Gillan, *Phys. Rev. Lett.* 80 (1998) 762.
- [13] E.V. Stefanovich, T.T. Truong, *Chem. Phys. Lett.* 299 (1999) 623.
- [14] W. Langel, *Surf. Sci.* 496 (2002) 141.
- [15] C. Zhang, P.J.F. Lindan, *J. Chem. Phys.* 118 (2003) 4620.
- [16] M. Menetrey, A. Markovits, C. Minot, *Surf. Sci.* 524 (2003) 49.
- [17] C. Zhang, P.J.D. Lindan, *J. Chem. Phys.* 121 (2004) 3811.
- [18] L.A. Harris, A.A. Quong, *Phys. Rev. Lett.* 93 (2004) 086105.
- [19] A.V. Bandura, D.G. Sykes, V. Shapovalov, T.N. Troung, J.D. Kubicki, R.A. Evarestov, *J. Phys. Chem. B* 108 (2004) 7844.
- [20] P.J.D. Lindan, C. Zhang, *Phys. Rev. Lett.* 95 (2005) 029601.
- [21] L.A. Harris, A.A. Quong, *Phys. Rev. Lett.* 95 (2005) 029602.
- [22] D.I. Sayago, M. Polcik, R. Lindsay, J.T. Hoeft, M. Kittel, R.L. Toomes, D.P. Woodruff, *J. Phys. Chem. B* 108 (2004) 14316.
- [23] D.P. Woodruff, A.M. Bradshaw, *Rep. Prog. Phys.* 57 (1994) 1029.
- [24] F. Allegretti, S. O'Brien, M. Polcik, D.I. Sayago, D.P. Woodruff, *Phys. Rev. Lett.* 95 (2005) 226104.
- [25] K.J.S. Sawhney, F. Senf, M. Scheer, F. Schäfers, J. Bahrtdt, A. Gaupp, W. Gudat, *Nucl. Instrum. Methods A* 390 (1997) 395.
- [26] L.-Q. Wang, D.R. Baer, M.H. Engelhard, A.N. Shultz, *Surf. Sci.* 344 (1995) 237.
- [27] K. Andersson, A. Nikitin, L.G.M. Pettersson, A. Nilsson, H. Ogasawara, *Phys. Rev. Lett.* 93 (2005) 196101.
- [28] J. Weissenrieder, A. Mikkelsen, J.N. Andersen, P.J. Feibelman, G. Held, *Phys. Rev. Lett.* 93 (2005) 196102.
- [29] C. Clay, S. Haq, A. Hodgson, *Phys. Rev. Lett.* 92 (2004) 046102.
- [30] H. Ogasawara, B. Brena, D. Nordlund, M. Nyberg, A. Pelmenschikov, L.G.M. Pettersson, A. Nilsson, *Phys. Rev. Lett.* 89 (2002) 276102.
- [31] R.L. Kurtz, R. Stockbauer, T.E. Madey, E. Román, J.L. de Segovia, *Surf. Sci.* 218 (1989) 178.
- [32] P.J.D. Lindan, C. Zhang, *Phys. Rev. B* 72 (2005) 075439.
- [33] V. Fritzsche, *J. Phys.: Condens. Matter* 2 (1990) 1413.
- [34] V. Fritzsche, *Surf. Sci.* 265 (1992) 187.
- [35] V. Fritzsche, *Surf. Sci.* 213 (1989) 648.
- [36] J.B. Pendry, *J. Phys. C: Solid State Phys.* 13 (1980) 937.
- [37] N.A. Booth, R. Davis, R. Toomes, D.P. Woodruff, C. Hirschmugl, K.-M. Schindler, O. Schaff, V. Fernandez, A. Theobald, Ph.

- Hofmann, R. Lindsay, T. Giessel, P. Baumgärtel, A.M. Bradshaw, Surf. Sci. 387 (1997) 152.
- [38] G. Charlton, P.B. Howes, C.L. Nicklin, P. Steadman, J.S.G. Taylor, C.A. Muryn, S.P. Harte, J. Mercer, R. McGrath, D. Norman, T.S. Turner, G. Thornton, Phys. Rev. Lett. 78 (1997) 495.
- [39] R. Lindsay, A. Wander, A. Ernst, B. Montanari, G. Thornton, N.M. Harrison, Phys. Rev. Lett. 94 (2005) 246102.
- [40] P. Baumgärtel, R. Lindsay, T. Giessel, O. Schaff, A.M. Bradshaw, D.P. Woodruff, J. Phys. Chem. B 104 (2000) 3044.
- [41] R. Dippel, K.-U. Weiss, K.-M. Schindler, D.P. Woodruff, P. Gardner, V. Fritzsche, A.M. Bradshaw, M.C. Asensio, Surf. Sci. 287/288 (1993) 465.
- [42] S. Andersson, J.B. Pendry, Solid State Commun. 16 (1975) 563.
- [43] V. Fritzsche, K.-M. Schindler, P. Gardner, A.M. Bradshaw, M.C. Asensio, D.P. Woodruff, Surf. Sci. 269/270 (1992) 35.
- [44] P. Reinhardt, B.A. Hess, Phys. Rev. B 50 (1994) 12015.
- [45] D. Vogtenhuber, R. Podloucky, A. Neckel, S.G. Steinemann, A.J. Freeman, Phys. Rev. 49 (1994) 2099.
- [46] M. Ramamoorthy, D. Vanderbilt, R.D. King-Smith, Phys. Rev. B 49 (1994) 16721.
- [47] P.J.D. Lindan, N.M. Harrison, M.J. Gillan, J.A. White, Phys. Rev. B 55 (1997) 15919.
- [48] S.P. Bates, G. Kresse, M.J. Gillan, Surf. Sci. 385 (1997) 386.
- [49] N.M. Harrison, X.-G. Wang, J. Muscat, M. Scheffler, Faraday Disc. 114 (1999) 305.
- [50] V. Swamy, J. Muscat, J.D. Gale, N.M. Harrison, Surf. Sci. 504 (2002) 115.
- [51] J.-T. Hoefl, M. Kittel, M. Polcik, S. Bao, R.L. Toomes, J.-H. Kang, D.P. Woodruff, M. Pascal, C.L.A. Lamont, Phys. Rev. Lett. 87 (2001) 086101.
- [52] G. Pacchioni, C. Di Valentin, D. Dominguez\_Ariza, F. Illas, T. Bredow, T. Klüner, V. Staemmler, J. Phys.: Condens. Matter 16 (2004) S2497.